Supporting Information

Fluorescent Polymer Nanoparticles Containing Perylene Diimides for Application in Luminescent Solar Concentrators

Rehana Pervin,[a] Elham M Gholizadeh,[a] Kenneth P. Ghiggino[a] and Wallace W. H. Wong*[a]

a. ARC Centre of Excellence in Exciton Science, School of Chemistry, The University of Melbourne, VIC 3052, Australia.

Email: wwhwong@unimelb.edu.au

Table of Contents

1. Dye Synthesis

Synthesis descriptions of PDI monomers

Synthesis of bPDI-donor

The bPDI-donor monomer was synthesized through a multi-step process (**Scheme S1**). Initially, tetrabutyl perylene-3,4,9,10-tetracarboxylate **1** was subjected to imidization with 2,6-dibromo-4-butylaniline, resulting in the formation of compound **2,** with yields of 13%. Compound **2** was the subjected to Suzuki coupling with 3,5-di-tert-butylphenylboronic acid, leading to the formation of compound 3 with a yield of 38%. Subsequently, compound **3** was refluxed in toluene with catalytic p-toluenesulfonic acid (TsOH) to generate the acid anhydride **4**. The yield for this step was moderate at 31%. Compound 4 was further reacted with 5-amino-1-pentanol in toluene, resulting in the formation of the intermediate 5 with a high yield of 85%. Finally, compound 5 was esterified with methacrylic acid to produce the desired **bPDI-donor** product with a yield of 65%.

Synthesis of bPDI-emitter

The synthesis of bPDI-emitter was carried out by 3 steps reactions (**Scheme S2**). In the first step, tetrachloroperylene tetracarboxylic acid dianhydride **(6)** was imidized with 2,6-diisopropylaniline and 5-amino-1-pentanol, resulting in the formation of compound **7** with a yield of 19%. In the second step, phenol was introduced in the bay position of PDI with **7** in the presence of K_2CO_3, yielding compound **8** with a yield of 47%. Finally, esterification of **8** with methacrylic acid at room temperature resulted in the desired **bPDI-emitter** product with 51% yield.

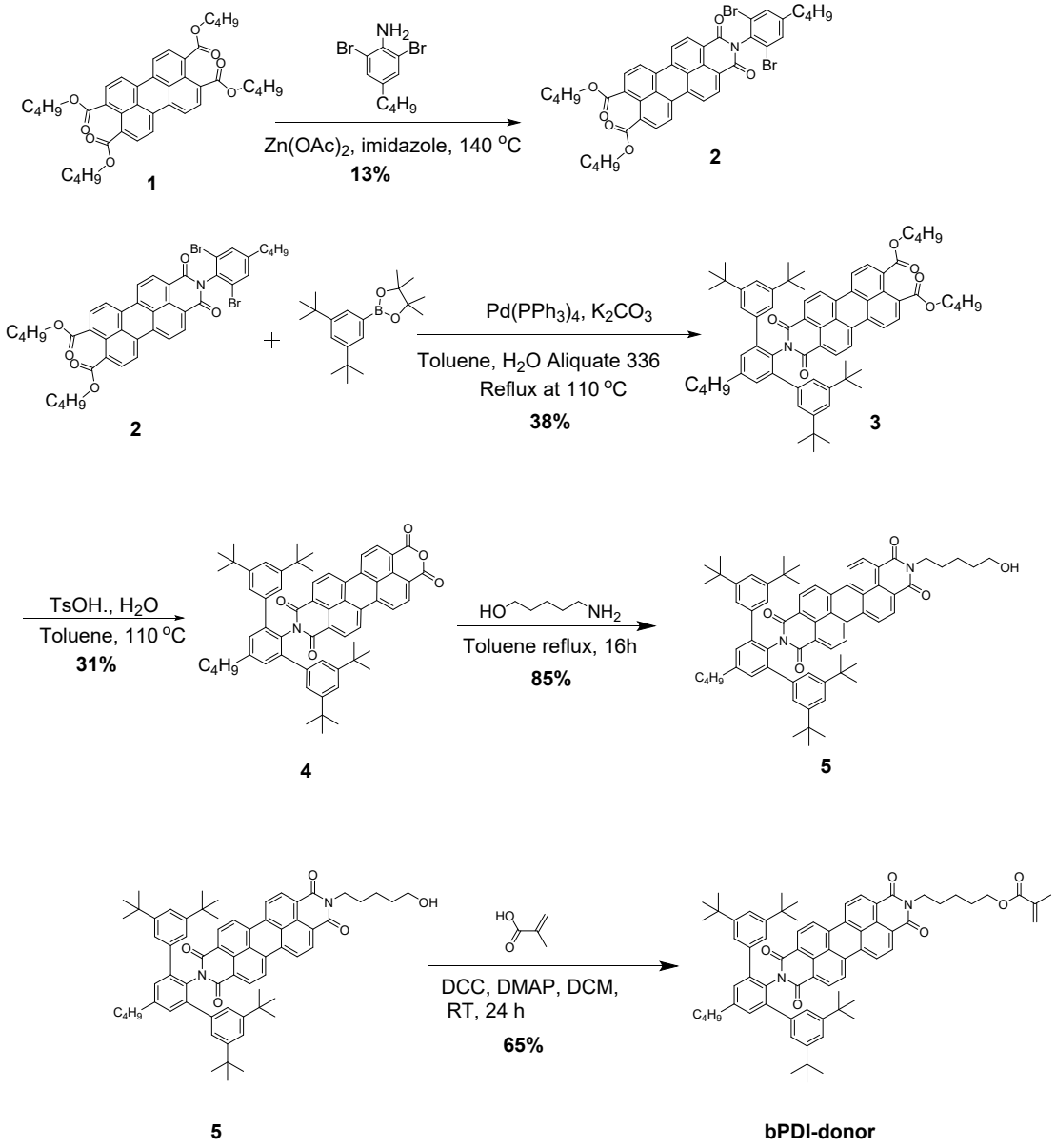

Scheme S1. Synthesis steps of bPDI-donor monomer.

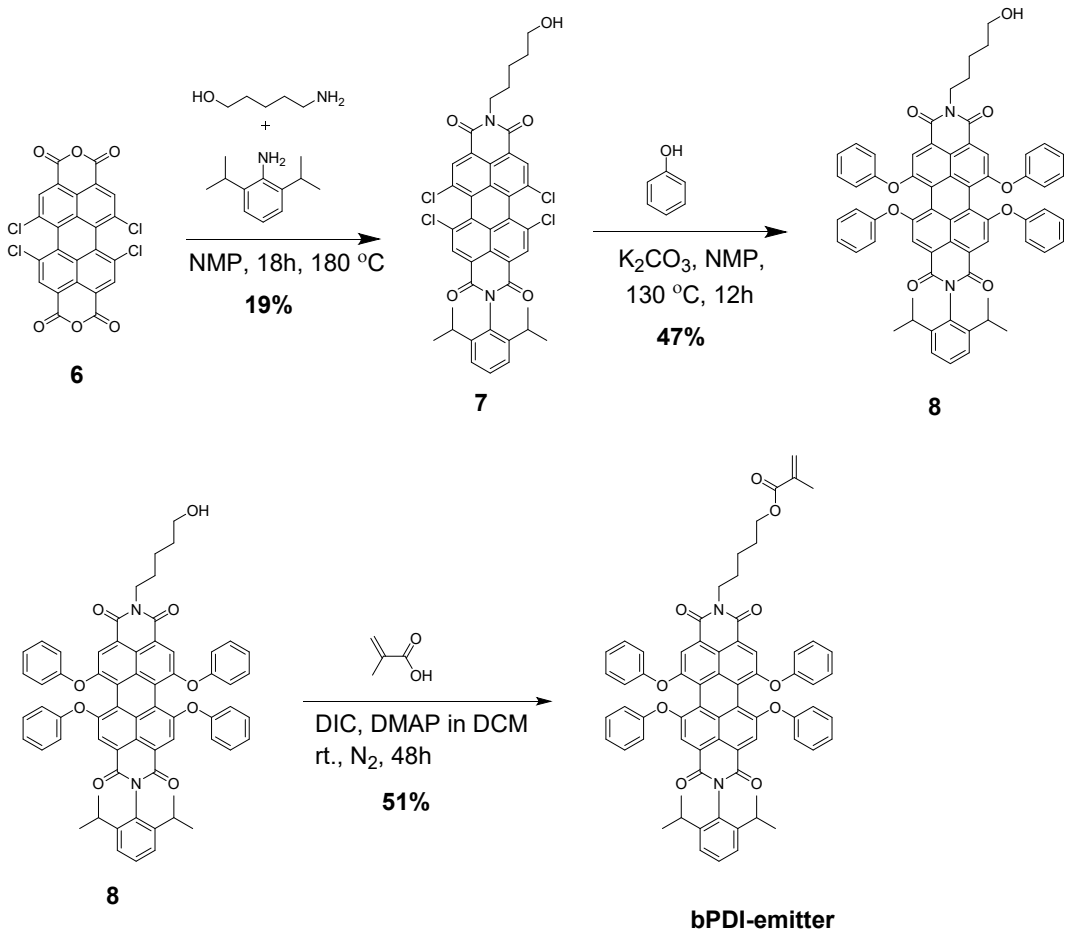

Scheme S2. Synthesis steps of bPDI-emitter monomer.

Detailed synthesis procedures

The tetrabutyl perylene-3,4,9,10-tetracarboxylate **(1)** was synthesized according to a literature procedure.[1, 2] 2,6-dibromo-4-butylaniline was synthesized according to a literature procedure.[3]

Dibutyl 2-(2,6-dibromo-4-butylphenyl)-1,3-dioxo-2,3-dihydro-1H-benzo[10,5]anthra[2,1,9-def]isoquinoline-8,9-dicarboxylate (2)

Imidazole (3 g, 44 mmol), tetrabutyl perylene-3,4,9,10-tetracarboxylate (**1**) (1 g, 1.53 mmol), 2,6-dibromo-4-butylaniline (1.4 g, 4.6 mmol) and catalytic amount of $Zn(OAc)_2$ (28 mg , 0.153 mmol) were added in a 30 ml Schlenk flask under N_2 atmosphere. The mixture was then heated at 140 °C and stirred for 12hours. The resulting red slurry was cooled to room temperature and diluted with chloroform while stirring. The crude was washed with H_2O to remove the imidazole and finally purified the product by flash chromatography ($CHCl_3$) to separate the target product (red orange powder, 190mg, yield 13 %). TLC ($CHCl_3$): R_f = 0.40

^{1}H NMR (600 MHz, Chloroform-*d*) δ 8.61 (d, *J* = 8.0 Hz, 2H), 8.32 (d, *J* = 8.1 Hz, 2H), 8.24 (d, *J* = 7.9 Hz, 2H), 7.98 (d, *J* = 7.9 Hz, 2H), 7.56 (s, 2H), 4.37 (t, *J* = 6.9 Hz, 4H), 2.67 (t, 2H), 1.88 – 1.78 (m, 4H), 1.72 – 1.63 (m, 2H), 1.57 – 1.47 (m, 4H), 1.47 – 1.37 (m, 2H), 1.02 (t, *J* = 7.4 Hz, 6H), 0.98 (t, *J* = 7.4 Hz, 3H). ^{13}C NMR (151 MHz, $CDCl_3$) δ 168.2, 162.2, 147.0, 136.1, 132.4, 132.1, 132.1, 132.1, 131.8, 130.3, 130.1, 129.1, 129.0, 126.3, 123.7, 122.8, 121.8, 121.8, 65.6, 34.9, 32.9, 30.6, 22.3, 19.3, 13.8, 13.8. MS ESI+ (m/z): calcd. for [M+H+] $C_{42}H_{38}Br_2NO_6$, 812.10399; found [M+H+], 812.10394.

[Dibutyl 1,3-dioxo-2-(3,3'',5,5''-tetra-tert-butyl-5'-butyl-[1,1':3',1''-terphenyl]-2'-yl)-2,3-dihydro-1H-benzo[10,5]anthra[2,1,9 def]isoquinoline-8,9-dicarboxylate] (3)

A mixture of perylene monoimide bisbutyl ester (**3-2**) (810 mg, 1 mmol), diisopropylphenyl boronic acid pinacol ester (950mg, 3 mmol) and $Pd(PPh_3)_4$ (110mg, 0.1mmol) were dissolved in degassed toluene (25ml, 8% w/w Aliquat 336) and 2M K_2CO_3 (in water) solution. This solution mixture was sealed under N_2 pressure, heated to 110 °C and stirred for 48h. After completing the reaction, the crude organic layer was separated and purified by flash chromatography (toluene) to separate the target product (red powder, 390mg, yield 37.8%). TLC (Toluene): R_f = 0.4

^{1}H NMR (600 MHz, Chloroform-*d*) δ 8.41 – 8.38 (m, 4H, PDI-Ar), 8.35 (d, *J* = 8.1 Hz, 2H), 8.08 (d, *J* = 7.9 Hz, 2H), 7.37 (s, 2H), 7.24 (d, *J* = 1.8 Hz, 4H), 7.09 (t, *J* = 1.9 Hz, 2H), 4.34 (t, *J* = 6.8 Hz, 4H), 2.85 – 2.74 (m, 2H), 1.83 – 1.72 (m, 6H), 1.54 – 1.42 (m, 6H), 1.09 (s, 36H), 1.00 (td, *J* = 7.4, 2.4 Hz, 9H). ^{13}C NMR (151 MHz, Chloroform-*d*)) δ 168.3, 163.5, 149.9, 143.6, 142.2, 138.7, 135.3, 132.4, 131.8, 131.2, 130.4, 129.7, 129.5, 129.4, 129.4, 129.3, 127.7, 125.9, 123.1, 122.5, 122.5, 122.3, 122.3, 121.7, 120.6, 65.6, 35.7, 34.7, 33.3, 31.6, 30.7, 22.8, 19.3, 14.1, 13.9. MS ESI+ (m/z): calcd. for [M+H+] $C_{70}H_{80}NO_6$, 1030.59802; found [M+H+], 1030.59806.

9-(3,3'',5,5''-Tetra-tert-butyl-5'-butyl-[1,1':3',1''-terphenyl]-2'-yl)-1H-isochromeno[6',5',4':10,5,6]anthra[2,1,9-def]isoquinoline-1,3,8,10(9H)-tetraone (4)

In a Schlenk flask a mixture of diester-PDI (**3**) (1.4g, 1.4 mmol), TsOH-H_2O (400mg, 2.1 mmol) were dissolved in dry toluene (28ml). The flask was connected by N_2 pressure, heated to 110 °C and stirred overnight. The crude product was purified by flush chromatography ($CHCl_3$: ethyl acetate 9:1) to separate the target product. Finally, the product was re-crystallized in toluene and methanol (red powder, 379 mg, yield 31%). This compound was used for the next step without further purification. TLC ($CHCl_3$: ethyl acetate 9:1): R_f = 0.6

^{1}H NMR (600 MHz, Chloroform-*d*) δ 8.68 (d, *J* = 8.0 Hz, 2H), 8.59 (d, *J* = 8.1 Hz, 2H), 8.52 (d, *J* = 8.1 Hz, 2H), 8.47 (d, *J* = 8.0 Hz, 2H), 7.36 (s, 2H), 7.21 (d, *J* = 1.9 Hz, 4H), 7.07 (t, *J* = 1.7 Hz, 2H), 2.81 – 2.77 (m, 2H), 1.79 – 1.73 (m, 2H), 1.51 – 1.47 (m, 2H), 1.07 (s, 36H), 0.99 (t, *J* = 7.3 Hz, 3H). ^{13}C NMR (101 MHz, Chloroform-*d*)) δ 163.1, 160.1, 150.0, 143.9, 142.1, 138.6, 136.5, 133.6, 131.2, 129.8, 129.3, 129.1, 126.9, 126.4, 124.1, 123.7, 123.2, 123.0, 120.7, 120.6, 120.4, 119.0, 35.7, 34.8, 33.3, 31.3, 22.8, 14.1. MS ESI+ (m/z): calcd. for [M+H$^+$] $C_{62}H_{62}NO_5$, 900.46225; found [M+H$^+$], 900.46224.

2-(5-Hydroxypentyl)-9-(3,3'',5,5''-tetra-tert-butyl-5'-butyl-[1,1':3',1''-terphenyl]-2'-yl)anthra[2,1,9-def:6,5,10-d'e'f']diisoquinoline-1, 3,8,10(2H,9H)-tetraone (5)

A mixture of **compound 4** (0.51g, 0.56mmol), 5-amino-1-pentanol (3eq. 176 mg, 1.7 mmol) and toluene (25 ml) were taken into a microtube under and refluxed with stirring for overnight. After completing the reaction, toluene was evaporated and the crude product was purified by flush chromatography in chloroform to give the target product (dark reddish powder, 529 mg, yield 90%). TLC (chloroform): R_f = 0.5

^{1}H NMR (500 MHz, Chloroform-*d*) δ 8.64 (d, *J* = 8.0 Hz, 2H), 8.54 (d, *J* = 8.1 Hz, 2H), 8.48 (d, *J* = 8.1 Hz, 2H), 8.44 (d, *J* = 8.0 Hz, 2H), 7.36 (s, 2H), 7.22 (d, *J* = 1.8 Hz, 4H), 7.07 (t, *J* = 1.9 Hz, 2H), 4.22 (dd, *J* = 8.4, 6.6 Hz, 2H), 3.68 (t, *J* = 6.4 Hz, 2H), 2.79 (t, 2H), 1.87 – 1.79 (m, 2H), 1.78 – 1.73 (m, 2H), 1.72 – 1.64 (m, 2H), 1.57 – 1.44 (m, 4H), 1.08 (s, 36H), 0.99 (t, *J* = 7.3 Hz, 3H). ^{13}C NMR (126 MHz, $cdcl_3$) δ 163.6, 163.4, 150.0, 143.8, 142.2, 138.7, 135.1, 134.4, 131.6, 131.3, 129.8, 129.5, 129.4, 129.3, 126.7, 126.3, 123.5, 123.2, 123.1, 123.0, 120.7, 120.6, 62.9, 40.6, 35.7, 34.8, 33.4, 32.5, 31.4, 28.0, 23.5, 22.9, 14.2. MS ESI+ (m/z): calcd. for [M+H+] $C_{67}H_{73}N_2O_5$, 985.55140; found [M+H+], 985.55139.

5-(1,3,8,10-Tetraoxo-9-(3,3'',5,5''-tetra-tert-butyl-5'-butyl-[1,1':3',1''-terphenyl]-2'-yl)-3,8,9,10-tetrahydroanthra[2,1,9-def:6,5,10-d'e'f']diisoquinolin-2(1H)-yl)pentyl methacrylate (bPDI-donor)

A mixture of compound **5** (256 mg, 0.26 mmol), methacrylic acid (10eq, 231.6 mg, 2.69 mmol), N,N'-Diisopropylcarbodiimide (DIC) (10eq, 339.4 mg, 2.69 mmol), and 4-dimethylaminopyridine (DMAP) (49.29 mg, 15 mol%) were taken into a microtube and continued the reaction in dichloromethane at room temperature at 24h under nitrogen flow. After completing the reaction, the white precipitate was filtered off and collected the filtrate and was further purified by flush chromatography in $CHCl_3$ to give the target product (orange solid, 183 mg, yield 64 %). TLC ($CHCl_3$): R_f = 0.45

^{1}H NMR (500 MHz, Chloroform-*d*) δ 8.64 (d, *J* = 7.9 Hz, 2H), 8.54 (d, *J* = 8.0 Hz, 2H), 8.48 (d, *J* = 8.1 Hz, 2H), 8.45 (d, *J* = 7.9 Hz, 2H), 7.37 (s, 2H), 7.23 (d, *J* = 1.8 Hz, 4H), 7.08 (t, *J* = 1.8 Hz, 2H), 6.13 – 6.07 (m, 1H), 5.58 – 5.51 (m, 1H), 2.80 (t, 2H), 1.87 – 1.69 (m, 6H), 1.55 (ddd, *J* = 12.7, 6.2, 3.5 Hz, 2H), 1.52 – 1.44 (m, 2H), 1.08 (s, 36H), 0.99 (t, *J* = 7.3 Hz, 3H). ^{13}C NMR (126 MHz, $cdcl_3$) δ 167.7, 163.6, 163.4, 150.0, 143.9, 142.3, 138.7, 136.7, 135.1, 134.5, 131.7, 131.3, 129.8, 129.6, 129.4, 126.7, 126.4, 125.5, 123.5, 123.3, 123.1, 123.1, 120.7, 114.7, 64.7, 43.1, 40.6, 35.8, 34.9, 33.4, 31.4, 28.6, 28.0, 23.8, 22.9, 18.6, 14.3. MS ESI+ (m/z): calcd. for [M+H+] $C_{71}H_{77}N_2O_6$, 1053.57761; found [M+H+], 1053.57764.

5,6,12,13-Tetrachloroanthra[2,1,9-def:6,5,10 d'e'f']diisochromene-1,3,8,10-tetraone (6)

Compound **6** was synthesized according to the modified literature procedure.[4] The starting material perylene-3,4,9,10-tetracarboxylic dianhydride (6.35mmol) was mixed with iodine (1.12 mmol) in chlorosulfonic acid (10 mL) and stirred at 65 °C for around 72 h. After that the hot solution was filtered by using glass wool to remove the insoluble starting materials and by- products. The filtrate was added dropwise into ice cold water while stirring and the resulting precipitate was

filtrated, washed with water generously. Finally dried in oven overnight. The product was an orange solid (3.08g, yield 91%) which is moderately soluble in chloroform. Due to the solubility issue the product was used in the next step without further purification.

^{1}H NMR (600 MHz, Chloroform-*d*) δ 8.75 (s, 4H).

5,6,12,13-Tetrachloro-2-(2,6-diisopropylphenyl)-9-(5-hydroxypentyl)anthra[2,1,9-def:6,5,10-d'e'f']diisoquinoline1,3,8,10(2H,9H)-tetraone (7)

A mixture of compound **6** (1 g, 1.8 mmol), 2,6-Diisopropylaniline (334.5 mg, 1.8 mmol), 5-amino-1-pentanol (193.9 mg, 1.8 mmol) were added in anhydrous 1-methyl-2-pyrrolidinone (NMP) (50 ml) and stirred at 180 °C under N_2 pressure for 18 h. Then, the reaction mixture was cooled to room temperature and poured into hydrochloric acid (50mL, 1 M). The precipitated orange product was filtered under suction, washed 3 times with water, and dried overnight under vacuum. Finally, crude product was purified by flush chromatography with DCM/MeOH (20:1) to give the dark red orange product (332.7 mg, yield 23 %).

(N.B. The compound was not perfectly pure. It was not possible to remove the impurities completely after doing several flash chromatography columns. The sample was used for the next reaction.) TLC (chloroform): R_f = 0.6

^{1}H NMR (600 MHz, Chloroform-*d*) δ 8.77 (s, 2H), 8.73 (s, 2H), 7.54 (t, *J* = 7.8 Hz, 1H), 7.39 (d, *J* = 7.8 Hz, 2H), 4.27 (t, 2H), 3.60 (t, *J* = 6.6 Hz, 2H), 2.85 – 2.69 (m, 2H), 2.00 – 1.86 (m, 2H), 1.69 – 1.57 (m, 2H), 1.21 (d, *J* = 7.7, 6.8 Hz, 12H). ^{13}C NMR (151 MHz, $CDCl_3$) δ 162.5, 145.9, 135.8, 133.6, 133.3, 129.2, 128.9, 124.5, 123.4, 63.0, 45.0, 41.0, 32.6, 29.5, 28.1, 24.2, 23.5. MS ESI+ (m/z): calcd. for [M+H+] $C_{41}H_{33}Cl_4N_2O_5$, 775.11086; found [M+H+], 775.11084.

2-(2,6-Diisopropylphenyl)-9-(5-hydroxypentyl)-5,6,12,13 tetraphenoxyanthra[2,1,9-def:6,5,10-d'e'f']diisoquinoline-1,3,8,10(2H,9H)-tetraone] (8)

A mixture of compound **7** (284mg, 0.36 mmol), phenol (512 mg, 5.86 mmol), and anhydrous K_2CO_3 (809 mg, 5.86 mmol) were added in anhydrous 1-methyl-2-pyrrolidinone (NMP) (15 ml) and stirred at 130 °C under N_2 pressure for 12h. Then, the reaction mixture was cooled to room temperature and poured into hydrochloric acid (20mL, 1 M) and stirred for another 1h at rt. The precipitated product was filtered under suction, washed 3 times with water, and dried under vacuum.

Finally, crude product was purified by flush chromatography with DCM/ MeOH (20:1) to give the expected product (dark purple fine powder, 150mg, yield 47%). TLC (chloroform): R_f = 0.6

^{1}H NMR (500 MHz, Chloroform-*d*) δ 8.22 (s, 2H), 8.17 (s, 2H), 7.39 (t, *J* = 7.8 Hz, 1H), 7.27 – 7.23 (m, 8H), 7.22 – 7.21 (m, 2H), 7.13 – 7.03 (m, 4H), 6.95 – 6.90 (m, 8H), 4.11 (t, *J* = 7.4 Hz, 2H), 3.60 (t, *J* = 6.5 Hz, 2H), 2.72 – 2.59 (m, 2H), 1.76 – 1.64 (m, 2H), 1.63 – 1.54 (m, 2H), 1.45 – 1.36 (m, 2H), 1.08 (d, *J* = 6.8 Hz, 12H). ^{13}C NMR (126 MHz, cdcl$_3$) δ 163.5, 163.3, 156.0, 155.9, 155.4, 155.4, 145.7, 133.1, 130.2, 130.1, 124.8, 124.7, 124.1, 123.0, 122.8, 121.0, 120.7, 120.5, 120.5, 120.2, 120.1, 120.0, 62.9, 40.6, 32.53, 29.2, 28.0, 24.2, 23.4. MS ESI+ (m/z): calcd. for [M+H+] $C_{65}H_{53}N_2O_9$, 1005.37456; found [M+H+], 1005.37463.

5-(9-(2,6-Diisopropylphenyl)-1,3,8,10-tetraoxo-5,6,12,13-tetraphenoxy-3,8,9,10-tetrahydroanthra[2,1,9-def:6,5,10-d'e'f']diisoquinolin-2(1H)-yl)pentyl methacrylate (bPDI-emitter)

A mixture of compound **8** (476 mg, 0.47 mmol), methacrylic acid (10eq. 407.5 mg, 4.73 mmol), N,N'-Diisopropylcarbodiimide (DIC) (10eq, 597 mg, 4.73 mmol), and 4-dimethylaminopyridine (DMAP) (86.6 mg, 15mol%) were taken into a microwave tube and continued the reaction in dichloromethane (60 ml) at room temperature at 48h under nitrogen flow. After completing the reaction, the white precipitate was filtered off and collected the filtrate. The crude product was further purified by flush chromatography in $CHCl_3$ to give the target product (dark red solid, 260 mg, yield 51 %). TLC (chloroform): R_f = 0.57

^{1}H NMR (500 MHz, Chloroform-*d*) δ 8.25 (s, 2H), 8.20 (s, 2H), 7.42 (t, *J* = 7.8 Hz, 1H), 7.30 – 7.27 (m, 8H), 7.25 – 7.24 (m, 2H), 7.16 – 7.05 (m, 4H), 6.99 – 6.92 (m, 8H), 6.08 – 6.04 (m, 1H), 5.53 – 5.47 (m, 1H), 4.18 – 4.07 (m, 4H), 2.78 – 2.59 (m, 2H), 1.90 (t, *J* = 1.3 Hz, 3H), 1.79 – 1.67 (m, 4H), 1.53 – 1.39 (m, 2H), 1.11 (d, *J* = 6.8 Hz, 12H). ^{13}C NMR (126 MHz, cdcl$_3$) δ 167.7, 163.5, 163.4, 156.1, 156.0, 155.5, 155.5, 145.8, 136.6, 130.2, 130.2, 125.5, 124.9, 124.8, 124.1, 123.0, 122.9, 121.0, 120.7, 120.6, 120.2, 120.2, 120.0, 64.7, 40.5, 29.3, 28.5, 27.9, 24.2, 23.7, 18.5. MS ESI+ (m/z): calcd. for [M+H+] $C_{69}H_{57}N_2O_{10}$, 1073.40077; found [M+H+], 1073.40076.

2. FRET data and calculations

Excitation Spectra

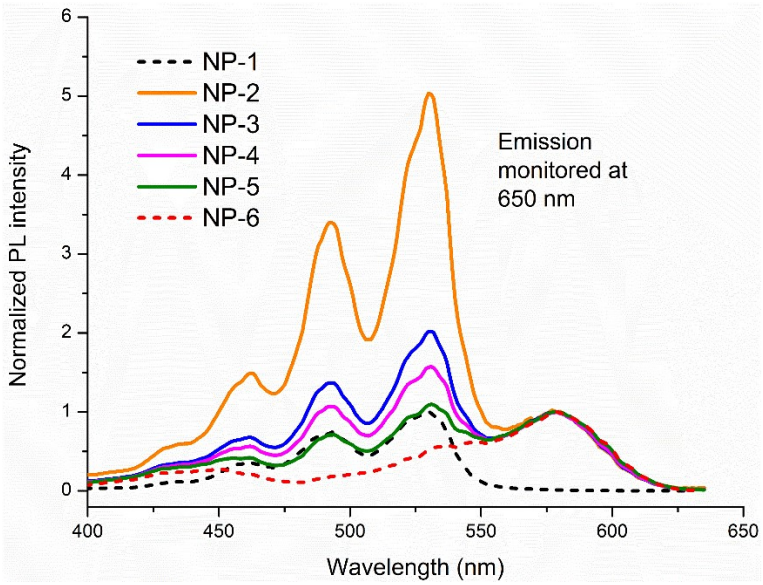

Figure S1. Excitation spectrum of nanoparticle samples dispersed in chloroform with emission monitored at 650 nm. The calculated FRET efficiency from this data for samples **NP-2** to **NP-5** are 80%, 65%, 51%, and 33%, respectively.

Calculation of the Förster radii (R_0) for the dyes

For an effective FRET process, proper alignment of the donor (D) and emitter (E) dipoles, spectral overlap between the emission spectrum of D and the absorption spectrum of E, and proximity between the donor and acceptor are crucial. The Förster's distance or critical distance (R_0, nm) is the molecular distance at which the energy transfer efficiency is 50%. R_0 can be calculated using the Förster equation.[5]

$$R_0 = 0.02108 \times \left(\frac{\kappa^2 \phi_{PLQY} J}{n^4}\right)^{\frac{1}{6}} \quad (1)$$

$$J = \int E_A(\lambda)\, F_D(\lambda) \lambda^4 \, d\lambda \quad (2)$$

where κ^2 is the orientation factor depending on dipole-dipole interaction (κ^2 = 2/3 for a randomly-oriented long lifetime donor-acceptor system), $\Phi_{PL\text{QY}}$ refers to the photoluminescence quantum efficiency of the donor in the absence of the emitter, and n is the refractive index of the matrix. The overlap integral, J ($nm^4\ M^{-1}\ cm^{-1}$), is a key factor that can be calculated from the overlap between the normalized area of the donor emission spectrum (F_D) and the emitter absorption spectrum expressed as the extinction coefficient (ε_A) over the full range of wavelengths λ.

In the present experimental setup, R_0 was calculated assuming the donor and emitter molecules have a random orientation, using κ^2 = 2/3 and n = 1.49 (PMMA) as parameters. For PDI-donor and PDI-emitter under these conditions, the calculated value for R_0 is 56.35 Å, and the overlap integral J is 2.21 x 10^{15} $nm^4\ M^{-1}\ cm^{-1}$.

Calculation of experimental energy transfer efficiency and estimation of donor-acceptor distance

The energy transfer efficiency depends on the critical energy transfer distance (R_0) and the average distance (r) between the donor and emitter, expressed by the following equation:

$$E = \frac{{R_0}^6}{{R_0}^6 + r^6} \tag{3}$$

The FRET efficiency, E, can be expressed using the previously developed method[6] as

$$E = \frac{A - X_A}{X_D} \tag{4}$$

Where *A* is the normalized excitation spectrum of the donor-emitter mixture sample, X_D is the normalized absorption spectrum of the donor and X_A is the normalized absorption spectrum of the acceptor.

3. *In situ* polymerization for making the bulk film

Figure S2 shows the custom-made mould used for fabrication of bulk films by *in situ* polymerization. Microscope glass slides (75 mm × 25 mm) were used as the front and back plates for the mold with a Teflon seal (2 mm thickness) sandwiched between the slides. The arrangement was clamped together using filing clips as pictured. After dispensing the NP-MMA mixture into the mold, the setup was placed in an oven at 70 °C for 24 hr. The resulting bulk film was then removed from the mold and cut into samples of 2.0 × 2.0× 0.2 cm^3.

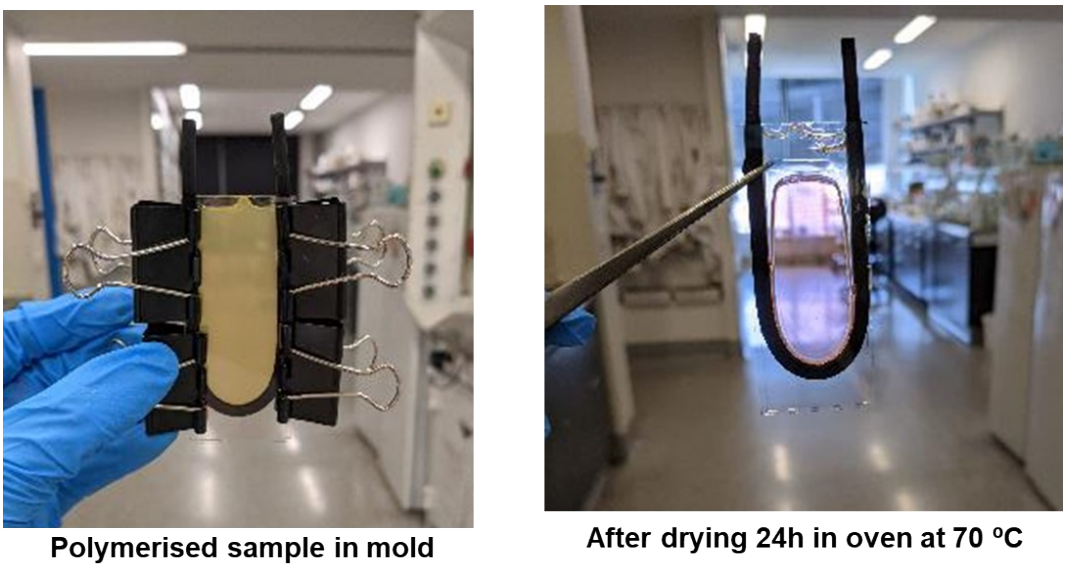

Figure S2. Fabrication of nanoparticle dispersed transparent bulk films.

4. Absolute photoluminescence quantum yield (Φ_{PL}) measurement

The absolute photoluminescence quantum yields (Φ_{PL}) of the materials both in solution and solid state were measured by using an integrating sphere (F3018, Horiba Jobin Yvon) on the FluorologOR -3 fluorometer. The excitation beam angle on the sample surface can be adjusted by changing the position of the sample holder (refer to **Figure S3**). The spectra for the Φ_{PL} of all the measurements were corrected for light source noise, wavelength sensitivity, and the use of transmittance filters. The photon counts for all the spectra measurements were limited to less than 2×10^6 cps to maintain the linear response of the detector. The Φ_{PL} measurements were conducted following previously reported procedures.[7] The Φ_{PL} was calculated using the following the equation:

$$\Phi_{PL} = \frac{I_{in}(\lambda) - (1-\alpha) I_{out}(\lambda)}{\alpha L_{blank,in}(\lambda)} \quad (5)$$

The symbol α represents the percentage of photons that are absorbed directly by the sample, with a correction made to account for secondary absorption from sphere-reflected photons.

$$\alpha = \frac{L_{out}(\lambda) - L_{in}(\lambda)}{L_{out}(\lambda)} \quad (6)$$

The emission intensity of the sample is represented by I_{in}, whereas I_{out} represents the emission intensity of the sample upon excitation by reflected light from the wall of the integrating sphere. $L_{blank;in}$ refers to the integrated excitation profile with the blank in the empty sphere. The emission intensity profiles were directly obtained from measurements. The excitation light intensity was determined by the number of photons counts from the scattering spectra across the excitation wavelength (± 5 nm).

The Φ_{PL} measurements for all donor materials used the re-absorption correction[8] technique, with the reference emission spectrum obtained from the Φ_{PL} sample without the integrating sphere. However, when reporting the Φ_{PL} values for all donor-acceptor systems, the re-absorption correction was not considered.

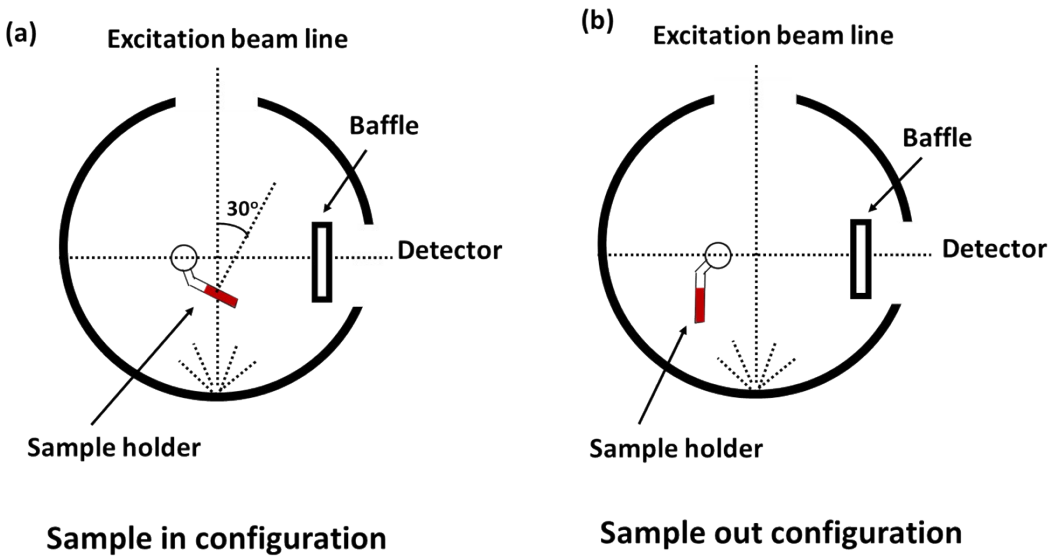

Figure S3. Sample configuration in the integrating sphere a) sample in the excitation beam line b) sample out in the excitation beamline.

5. Fluorescence decay experiments

To gain a deeper understanding of the FRET process in NPs-dispersed bulk films, the fluorescence decay of the donor was investigated using time-correlated single photon counting (TCSPC) measurements. The films were excited at 470 nm and the emission was monitored at 530 nm (donor emission wavelength). As depicted in **Figure S4**, the fluorescence decay profiles of the donor showed a significantly faster decay when the emitter was present, which could be attributed to non-radiative resonance-type energy transfer. The average lifetime of NPs containing only the donor (D (1wt%)) was 4.72 ns, and with the addition of various emitters, the lifetime of the donor gradually decreased. Furthermore, TCSPC analysis revealed several decay components for the D-E containing film (**Table S1**), which could be related to heterogeneity in the rates of energy transfer between the donor and the emitter. The luminophores are randomly distributed in the polymer chain, so it is likely that some donor-emitter luminophores are closer together, leading to faster decay, compared to others. The donor-only film also showed two decay components, including a long-lived 9.15 ns lifetime component (fi of 21.25%), which is likely due to weak excimer emission of the donor at high dye

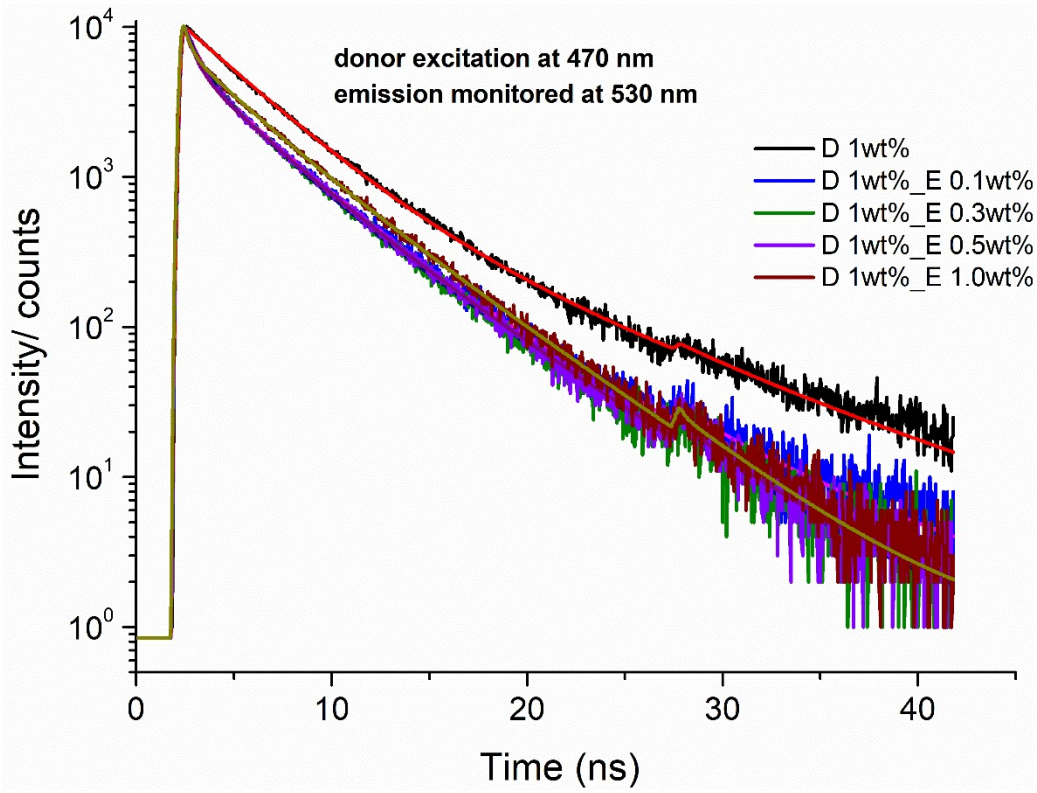

Figure S4. Lifetime decay profiles of the nanoparticles dispersed bulk films with various dye ratios (λ_{exi} 470nm and λ_{emi} 530 nm). Solid lines are fitted curves with values provided in Table S1.

concentrations. Excimer emission has been reported previously for PDI luminophores in film environments.[9]

Table S1. Analysis of TCSPC fluorescence decay data of the NPs dispersed bulk films. Excitation 470 nm, emission 530 nm

sample	τ_i /ns (f_i %)[a]	τ_{avg}/ns	χ^2
D 1wt%	3.49 (78.74), 9.15 (21.25)	4.72	1.42
D 1wt%_E 0.1wt%	0.70 (16.56), 3.53 (69.39), 7.67 (14.03)	3.61	1.16
D 1wt%_E 0.3wt%	0.6 (13.30), 2.57 (39.78), 4.99 (46.91)	3.44	1.13
D 1wt%_E 0.5wt%	0.52 (13.65), 2.96 (45.25), 5.20 (41.09)	3.54	1.00
D 1wt%_E 1.0wt%	0.31 (7.07), 2.82 (36.05), 4.85 (56.87)	3.79	1.03

[a]In brackets the fractional contribution of each decay component is given by, $f_i = 100 \times \frac{B_i \times \tau_i}{\sum B_i \times \tau_i}$ where B_i denotes the pre-exponential factor (or amplitude) of each lifetime.

The fluorescence decays of D-E monomer bulk films were also measured at the emitter wavelength of 625 nm following donor excitation at 470nm. In each case a sub-nanosecond risetime was required for adequate fitting of the data consistent with the presence of an energy transfer process populating the emitter. Detailed analysis of the decay data can be found in **Table S2**. The fluorescence decays exhibited a complex nature and are likely impacted by the heterogeneity in emitter environments and donor-emitter distances (**Figure S5**). A feature is a long decay component in the particles with a high donor concentration which might be attributed to excimer emission.

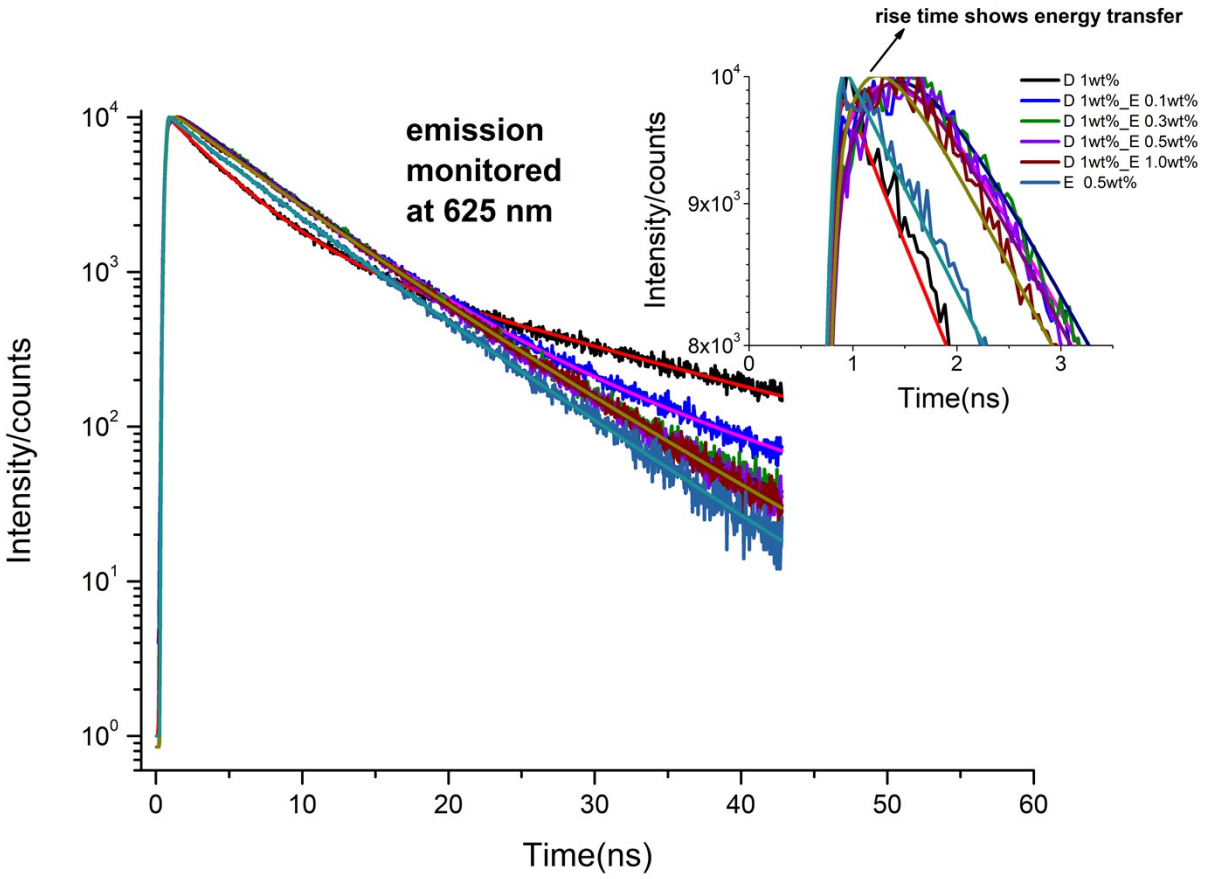

Figure S5. Fluorescence decay profiles of the D-E films monitoring emitter at 625 nm (excitation of donor at 470 nm). Inset shows evidence of a risetime at early times consistent with energy transfer.

Table S2. Analysis of TCSPC fluorescence decay data of the NPs dispersed bulk films. Excitation 470 nm, emission 625 nm

Sample	τ_i /ns (f_i %)[a]	τ_{avg}/ns	χ^2	Rise time/ns
D 1wt%_E 0.1wt%	0.49 (2.26), 5.88 (81.78), 16.31 (15.49)	7.34	1.13	0.49
D 1wt%_E 0.3wt%	0.45 (2.58), 6.18 (91.33), 16.97 (6.08)	6.68	1.21	0.45
D 1wt%_E 0.5wt%	0.37 (2.22), 5.93 (83.33), 10.81 (14.44)	6.51	1.22	0.37
D 1wt% _E 1.0wt%	0.26 (1.40), 5.39 (50.86), 8.22 (47.73)	6.66	1.14	0.26
E 0.5 wt%	4.37 (27.01), 7.07 (72.98)	6.34	1.16	-

[a]In brackets the fractional contribution of each decay component is given by, $f_i = 100 \times \frac{B_i \times \tau_i}{\sum B_i \times \tau_i}$ where B_i denotes the pre-exponential factor (or amplitude) of each lifetime.

6. Monte Carlo ray tracing simulations

A Monte-Carlo ray-tracing simulation[10-12] was conducted to predict the edge output performance of LSC devices, using the method and simulation program previously developed by Zhang et al.[13] The program operates under the assumption of the classical ray model of light, where light travels in a straight line until it encounters an interface or participating particle. Reflection, absorption, and transmission are all possible outcomes for a light ray. The program also assumes that the dye particles are uniformly distributed within the host matrix and are monodisperse, meaning they are not aggregated. During the simulation, all events such as re-absorption, reflection, escape cone loss, Φ_{PL} loss, or release from edges are monitored to assess the waveguide system's performance. However, scattering losses are not included in the simulation. The Monte-Carlo ray-tracing simulation process is depicted in **Figure S6**.

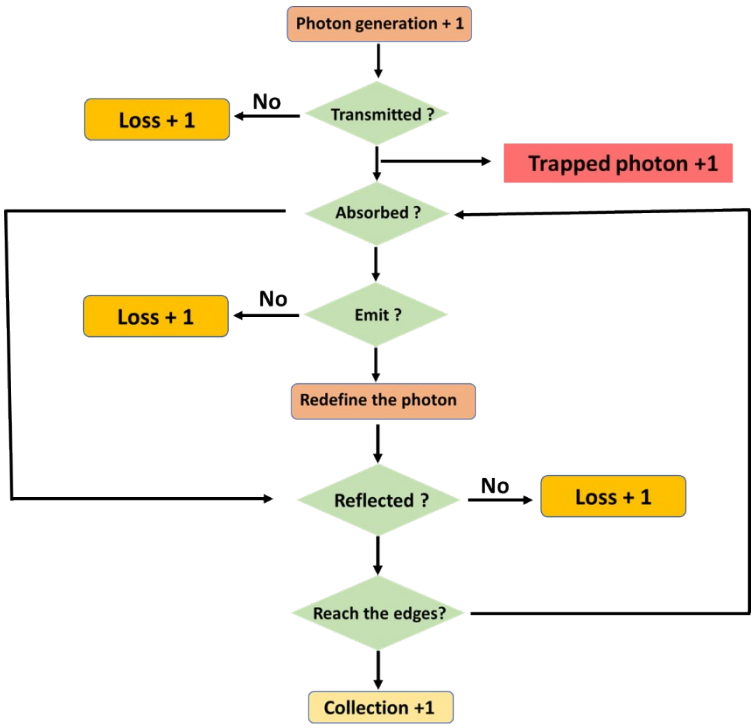

Figure S6. Flow chart of the Monte-Carlo ray tracing simulation process.

7. NMR spectra

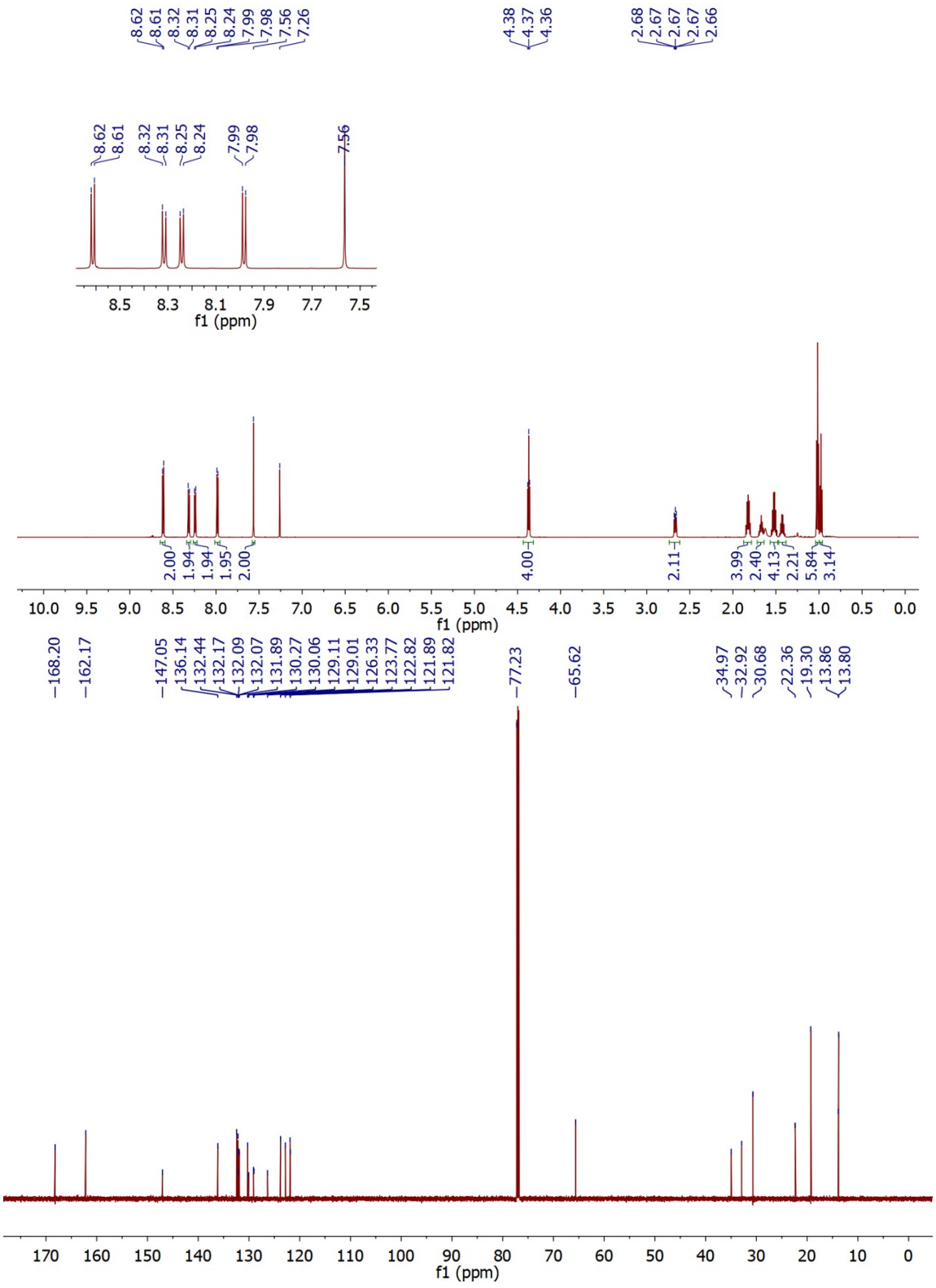

Figure S7. ^{1}H and ^{13}C-NMR spectrum of **2** in $CDCl_3$.

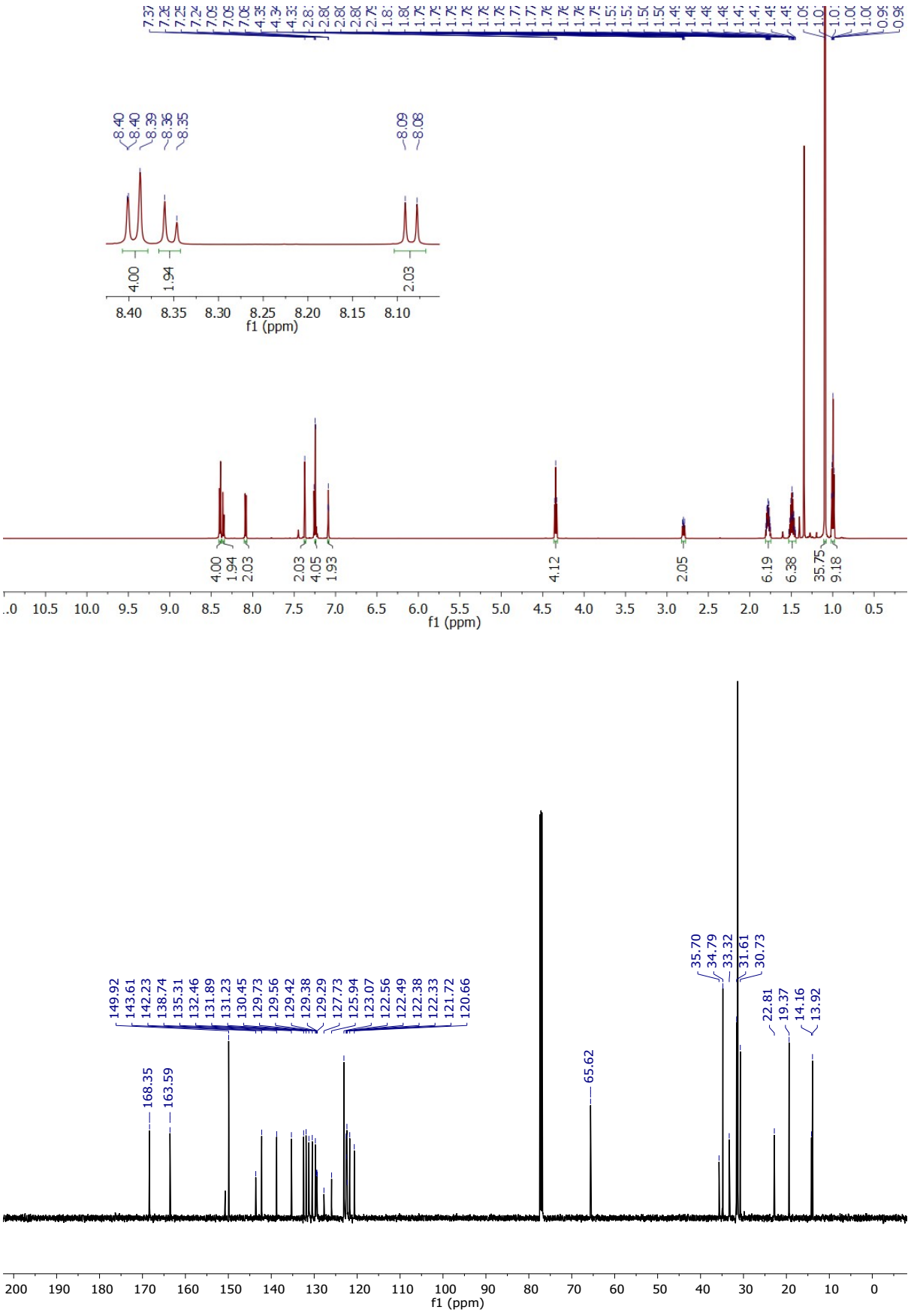

Figure S8. ^{1}H and ^{13}C-NMR spectrum of **3** in $CDCl_3$.

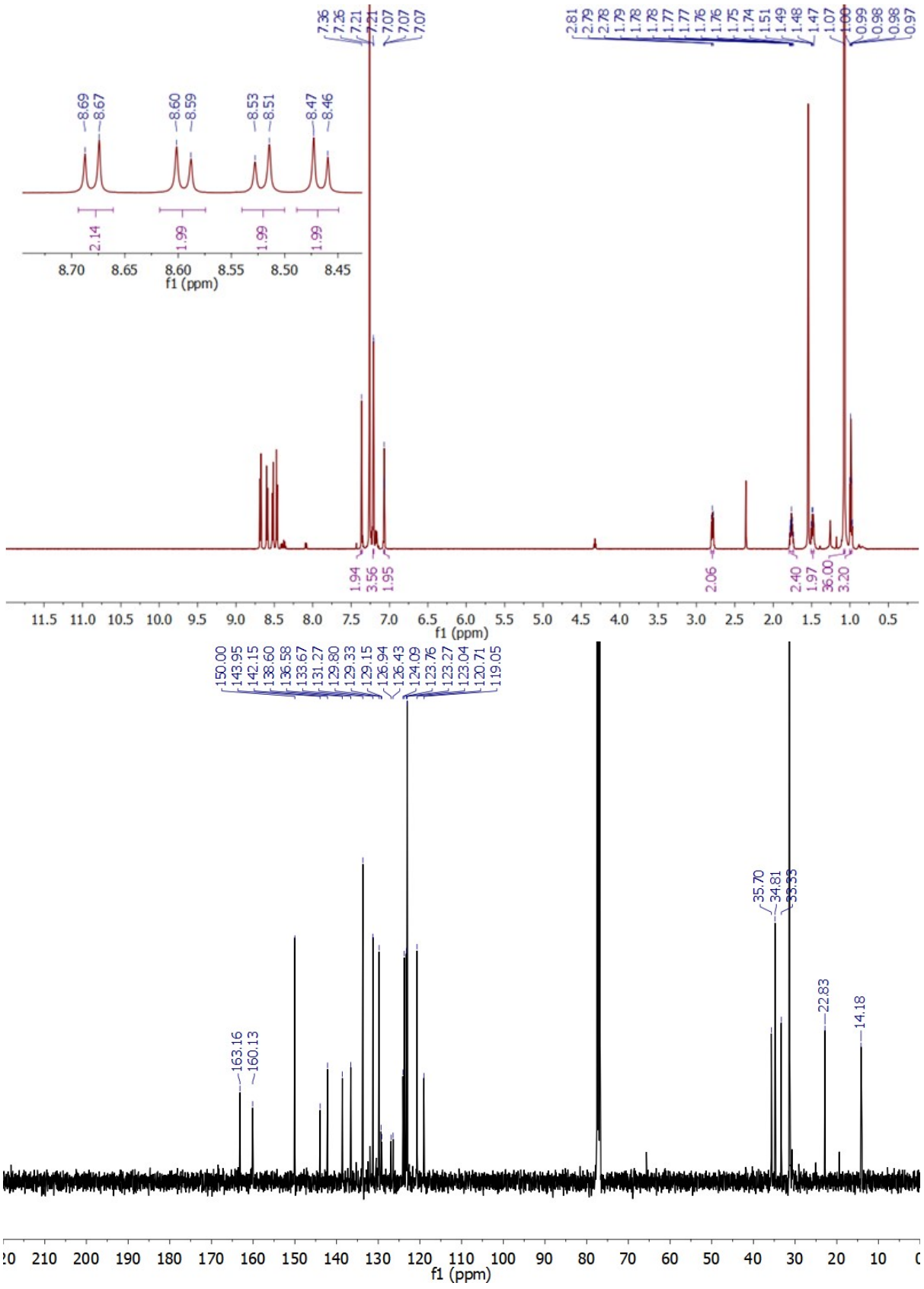

Figure S9. ^{1}H and ^{13}C-NMR spectrum of **4** in $CDCl_3$.

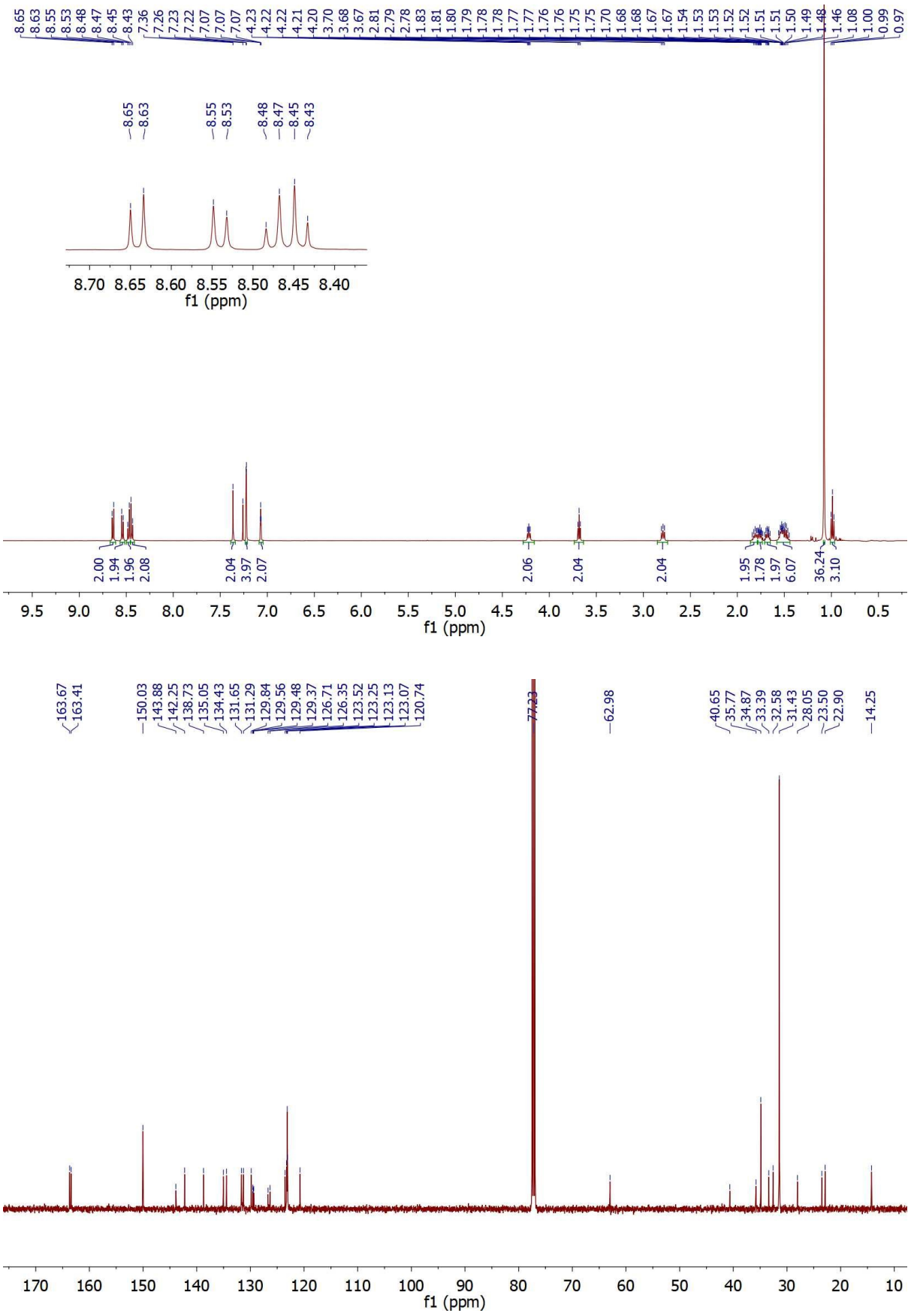

Figure S10. ^{1}H and ^{13}C-NMR spectrum of **5** in $CDCl_3$.

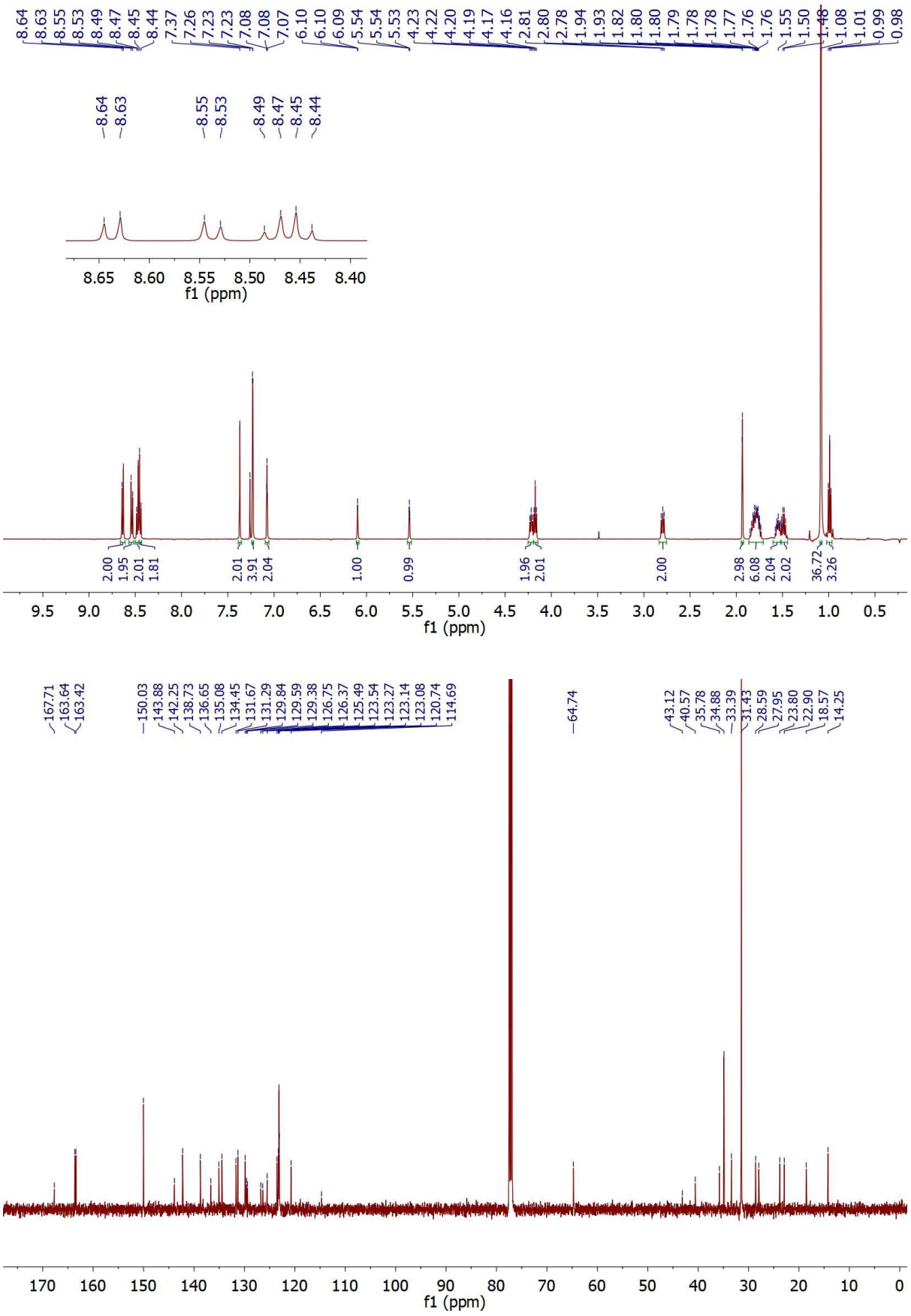

Figure S11. ^{1}H and ^{13}C-NMR spectrum of **bPDI-donor** in $CDCl_3$.

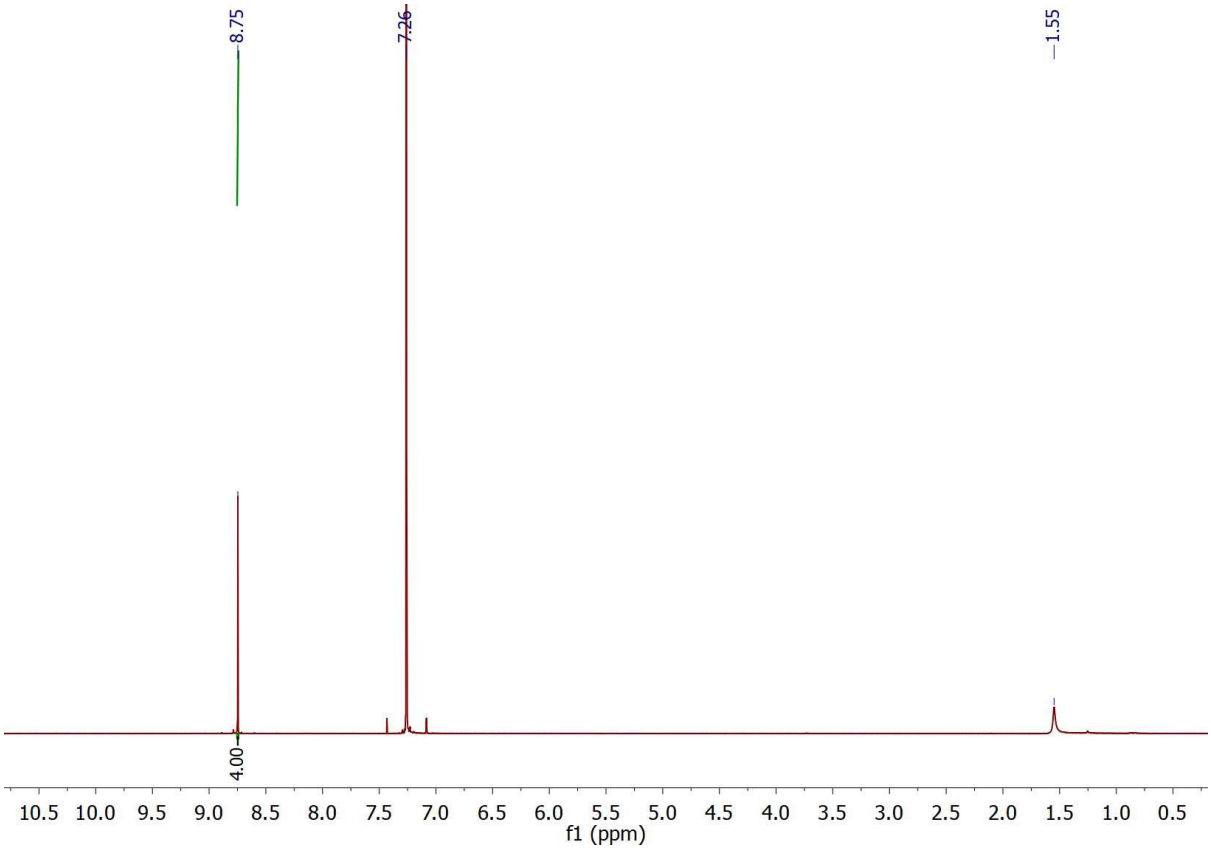

Figure S12. ^{1}H NMR spectrum of **6** in $CDCl_3$.

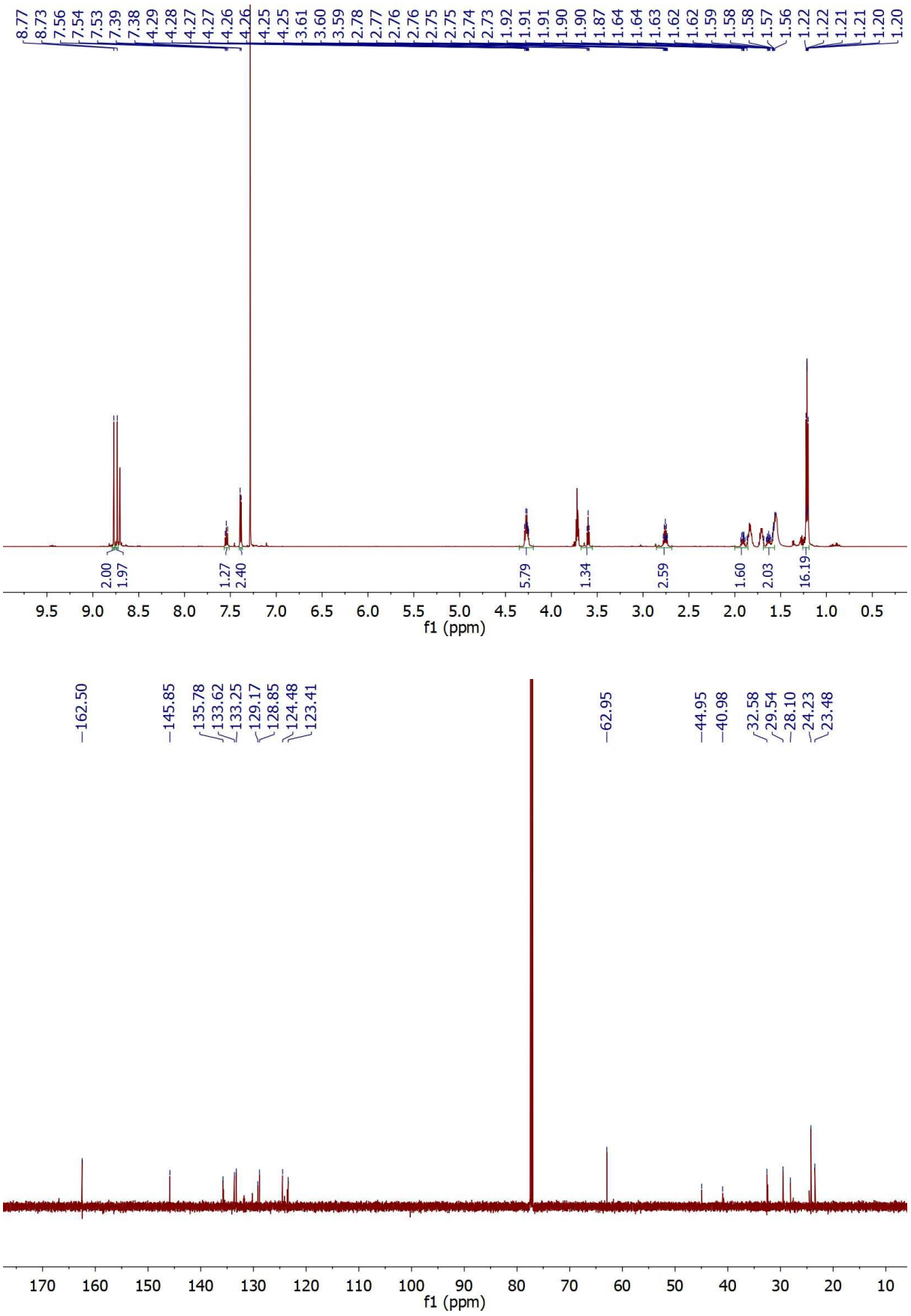

Figure S13. ^{1}H and ^{13}C-NMR spectrum of **7** in $CDCl_3$.

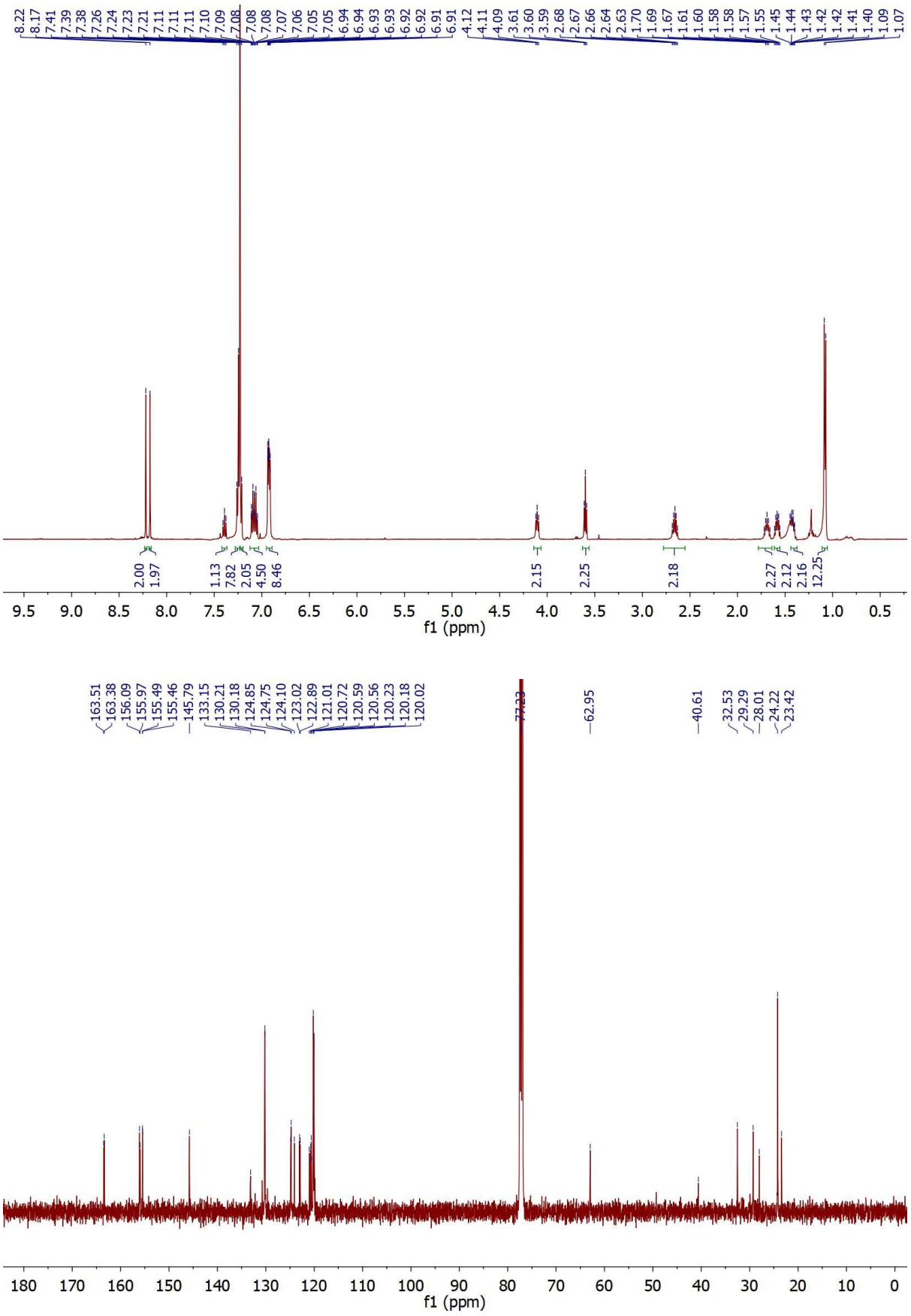

Figure S14. ^{1}H and ^{13}C-NMR spectrum of **8** in $CDCl_3$.

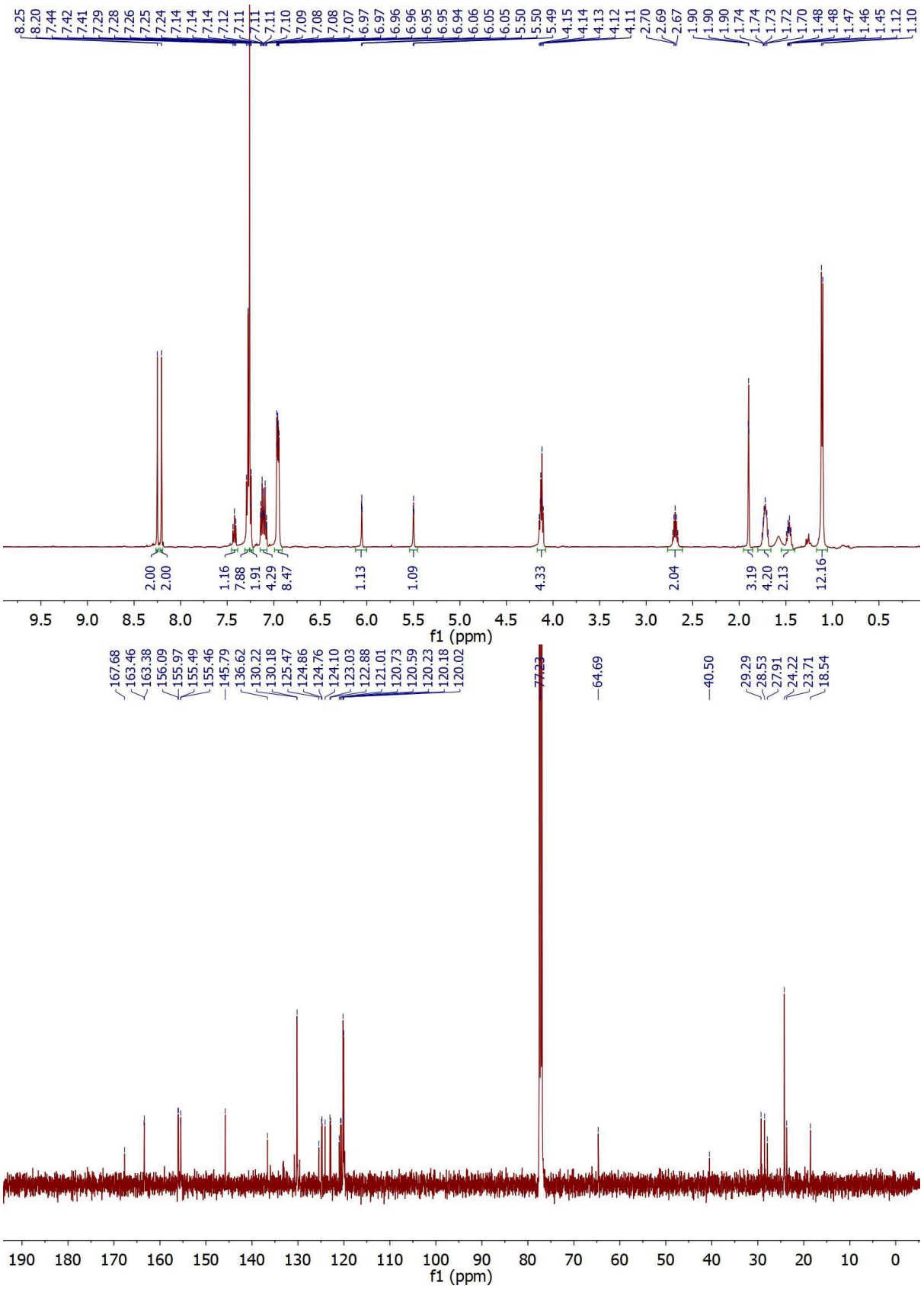

Figure S15. ^{1}H and ^{13}C-NMR spectrum of **bPDI-emitter** in $CDCl_3$.

8. References

1. J. A. Hutchison, H. Uji-i, A. Deres, T. Vosch, S. Rocha, S. Müller, A. A. Bastian, J. Enderlein, H. Nourouzi and C. Li, *Nat. Nanotechnol*, 2014, **9**, 131-136.
2. E. Verde-Sesto, M. Pintado-Sierra, A. Corma, E. M. Maya, J. G. de la Campa, M. Iglesias and F. Sánchez, *Chem. Eur. J.*, 2014, **20**, 5111-5120.
3. J. L. Banal, H. Soleimaninejad, F. M. Jradi, M. Liu, J. M. White, A. W. Blakers, M. W. Cooper, D. J. Jones, K. P. Ghiggino and S. R. Marder, *J. Phys. Chem. C*, 2016, **120**, 12952-12958.
4. B. E. Partridge, P. Leowanawat, E. Aqad, M. R. Imam, H.-J. Sun, M. Peterca, P. A. Heiney, R. Graf, H. W. Spiess and X. Zeng, *J. Am. Chem. Soc.*, 2015, **137**, 5210-5224.
5. A. Demchenko, *Introduction to fluorescence sensing*, 2009, 65-118.
6. L. Stryer and R. P. Haugland, *PNAS*, 1967, **58**, 719-726.
7. L. Porres, A. Holland, L.-O. Pålsson, A. P. Monkman, C. Kemp and A. Beeby, *J. Fluoresc.*, 2006, **16**, 267-273.
8. L. R. Wilson and B. S. Richards, *Appl. Opt.*, 2009, **48**, 212-220.
9. V. B. Yasarapudi, L. Frazer, N. J. Davis, E. P. Booker, A. Macmillan, J. K. Gallaher, D. Roberts, S. Perrier and T. W. Schmidt, *J. Mater. Chem. C*, 2018, **6**, 7333-7342.
10. H. Hernandez-Noyola, D. H. Potterveld, R. J. Holt and S. B. Darling, *Energy & Environmental Science*, 2012, **5**, 5798-5802.
11. M. Carrascosa, S. Unamuno and F. Agulló-López, *Appl. Opt.*, 1983, **22**, 3236-3241.
12. D. Şahin, B. Ilan and D. F. Kelley, *Journal of Applied Physics*, 2011, **110**, 033108.
13. B. Zhang, H. Yang, T. Warner, P. Mulvaney, G. Rosengarten, W. W. Wong and K. P. Ghiggino, *Methods Appl. Fluores.*, 2020, **8**, 037001.